International Journal of Mass Spectrometry 286 (2009) 104–111

Contents lists available at ScienceDirect

International Journal of Mass Spectrometry

journal homepage: www.elsevier.com/locate/ijms

Dissociation of fluorotoluene molecular ions: A theoretical study

Joong Chul Choe*

Department of Chemistry, Dongguk University, 3-26 Pil-Dong, Chung-gu, Seoul 100-715, Republic of Korea

ARTICLE INFO

Article history:
Received 8 June 2009
Received in revised form 28 June 2009
Accepted 6 July 2009
Available online 24 July 2009

Keywords:
Benzylium
Tropylium
DFT calculation
RRKM calculation
Substitution effect

ABSTRACT

The potential energy surfaces (PESs) for the isomerizations and dissociations of the α-, *o*-, *m*-, and *p*-fluorotoluene molecular ions were determined using density functional theory molecular orbital calculations. Rice–Ramsperger–Kassel–Marcus model calculations were carried out to understand the kinetics of the isomerizations and dissociations based on the PESs obtained. Kinetic analysis showed that the interconversion among the four molecular ions was much faster than the dissociations at low energies. The main product was a mixture of the fluorotropylium and *p*-fluorobenzylium ions formed by the loss of H$^\bullet$ in the dissociation of all of the molecular ions investigated. At high energies, the α-fluorobenzylium ion was another important product in the dissociation of the α-fluorotoluene ion. A fluorine substitution effect on the C–H bond dissociation energy was observed, which was well explained by the valence bond theory.

1. Introduction

The dissociation of halotoluene molecular ions has been extensively studied using a variety of experimental and theoretical methods [1–23]. These studies have been mainly devoted to the structural identification of the $C_7H_7^+$ products formed by the loss of a halogen, including the mechanistic dissociation pathways. The presence of four structural isomers (α-, *o*-, *m*-, and *p*-) makes the isomerization and dissociation pathways more complicated and, hence, more interesting than those of the toluene (TOL) molecular ion. It is well known that the benzylium (Bz^+) and tropylium (Tr^+) ions are formed from $TOL^{+\bullet}$ through direct C–H bond cleavage and ring expansion, respectively [24,25]. Recently, it was suggested that a rearrangement to the ionized *o*-isotoluene (5-methylene-1,3-cycloheptadiene) intermediate can contribute to the formation of Bz^+ [26]. One might easily expect the α-halotoluene (benzyl halide) molecular ions ($C_6H_5CH_2X^{+\bullet}$, X = Cl, Br, I) to undergo mechanistic pathways to form $C_7H_7^+$ products similar to $TOL^{+\bullet}$, as shown in our recent theoretical studies [15,16]. According to previous reports, the formation of Bz^+ is much more favored than that of Tr^+. In the dissociations of the *o*-, *m*-, and *p*-isomers, the major $C_7H_7^+$ products were assigned the benzylium structure both experimentally and theoretically [15–19,22]. It has been suggested that the halogenated isotoluene ions are important intermediates in the pathways leading to the formation of Bz^+.

Fluorotoluene molecular ions have attracted less attention than the other halotoluene ions mentioned above. According to previous experimental results, all four isomeric fluorotoluene ions lose H$^\bullet$ more easily than X$^\bullet$, whereas the opposite is true for the other halotoluene ions [4,8,27]. This is in line with the order of the C–H and C–X bond energies: C–F > C–H > C–Cl > C–Br > C–I. Therefore, the possible main product ions in the dissociations of the fluorotoluene ions are the fluorobenzylium (FBz^+) and fluorotropylium (FTr^+) ions rather than Bz^+ and Tr^+, respectively, and, hence, the mechanistic dissociation pathways would be different from those of the aforementioned halotoluene ions. In this work, the potential energy surfaces (PESs) for the dissociations of α-, *o*-, *m*-, and *p*-fluorotoluene molecular ions (**1a**, **2a**, **3a**, and **4a**, respectively) were obtained by density functional theory (DFT) calculations. Based on the PESs obtained, a kinetic analysis was carried out on their isomerizations and dissociations to reveal the main dissociation channels. From the similarity of the PESs to those associated with $TOL^{+\bullet}$, we will discuss the fluorine substitution effect on the C–H bond dissociation energy (BDE).

2. Computational methods

The molecular orbital (MO) calculations were performed using the Gaussian 03 suite of programs [28]. Geometry optimizations for the stationary points were carried out at the unrestricted B3LYP level of DFT using the 6-31G(d) basis set. The transition state (TS) geometries connecting the stationary points were searched and checked by calculating the intrinsic reaction coordinates at the same level. Single point energy calculations were carried out at the B3LYP/6-311+G(3df,2p) level to improve the

* Tel.: +82 2 2260 8914; fax: +82 2 2268 8204.
E-mail address: jcchoe@dongguk.edu.

1387-3806/$ – see front matter © 2009 Elsevier B.V. All rights reserved.
doi:10.1016/j.ijms.2009.07.007

accuracy of the energies. It has been suggested that the B3LYP/6-311 + G(3df,2p)//B3LYP/6-31G(d) calculations gives reliable total and reaction energies at 0 K for organic radical cations within ±6 kJ mol^{-1} [29]. The harmonic frequencies calculated at the B3LYP/6-31G(d) level and scaled by 0.9806 [30] were used for the zero point vibrational energy (ZPVE) corrections. To enhance the accuracy of the energies of the selected species, Gaussian-3 (G3) theory calculations using the B3LYP density functional method (G3//B3LYP) [31] were performed. In the G3//B3LYP calculations, the geometries are obtained at the B3LYP/6-31G(d) level, and the ZPVEs are obtained at the same level and scaled by 0.96. All of the other steps remain the same as those of the G3 method [32] with the exception of the values of the higher-level correction parameters.

The RRKM expression was used to calculate the rate-energy dependences as follows [33]:

$$k(E) = \frac{\sigma N^{\neq}(E - E_0)}{h\rho(E)}, \quad (1)$$

where E is the reactant internal energy, E_0 the critical energy of the reaction, $N^{\neq}$ the sum of the TS states, ρ the density of the reactant states, σ the reaction path degeneracy, and h is the Planck's constant. $N^{\neq}$ and ρ were evaluated by the direct count of the states using the Beyer–Swinehart algorithm [34].

3. Results and discussion

1a can produce α-FBz$^+$ by the direct cleavage of the C–H bond of the CH_2F group (Scheme 1a). Its endoergicity calculated at the B3LYP/6-311 + G(3df,2p)//B3LYP/6-31G(d) level was 173 kJ mol^{-1}, which was much smaller than that (237 kJ mol^{-1}) for the formation of Bz$^+$ by direct C–F bond cleavage. Alternatively, **1a** can produce FTr$^+$ by the well-known rearrangement to the seven-membered ring isomer, **1d**, (the so-called Hoffman mechanism [35]), followed by the loss of H$^\bullet$. Even though **1d** can lose F$^\bullet$ to form Tr$^+$, its energy barrier (135 kJ mol^{-1}) was higher than that (110 kJ mol^{-1}) for the loss of H$^\bullet$ from **1d**. Therefore, the calculations predict that the loss of H$^\bullet$ is more favored than the loss of F$^\bullet$ in the dissociation of **1a**, which is in agreement with the previous experimental results [27]. Similarly, each of the ions **2a**–**4a** can undergo either C–H bond cleavage to generate *o*-, *m*-, or *p*-FBz$^+$, or ring-expansion rearrangement followed by loss of H$^\bullet$ to yield FTr$^+$. The former reaction forms, respectively, and the latter reaction forms FTr$^+$. Alternatively, **2a**–**4a** can form *o*-, *m*-, and *p*-tolylium ions, respectively, by the direct cleavage of the C–F bond. However, their reaction endoergicities (448, 452, and 472 kJ mol^{-1}, respectively) were much larger than those (230, 240, and 224 kJ mol^{-1}, respectively) for the formations of *o*-, *m*-, and *p*-FBz$^+$. This excludes the possibility of tolylium ions being formed.

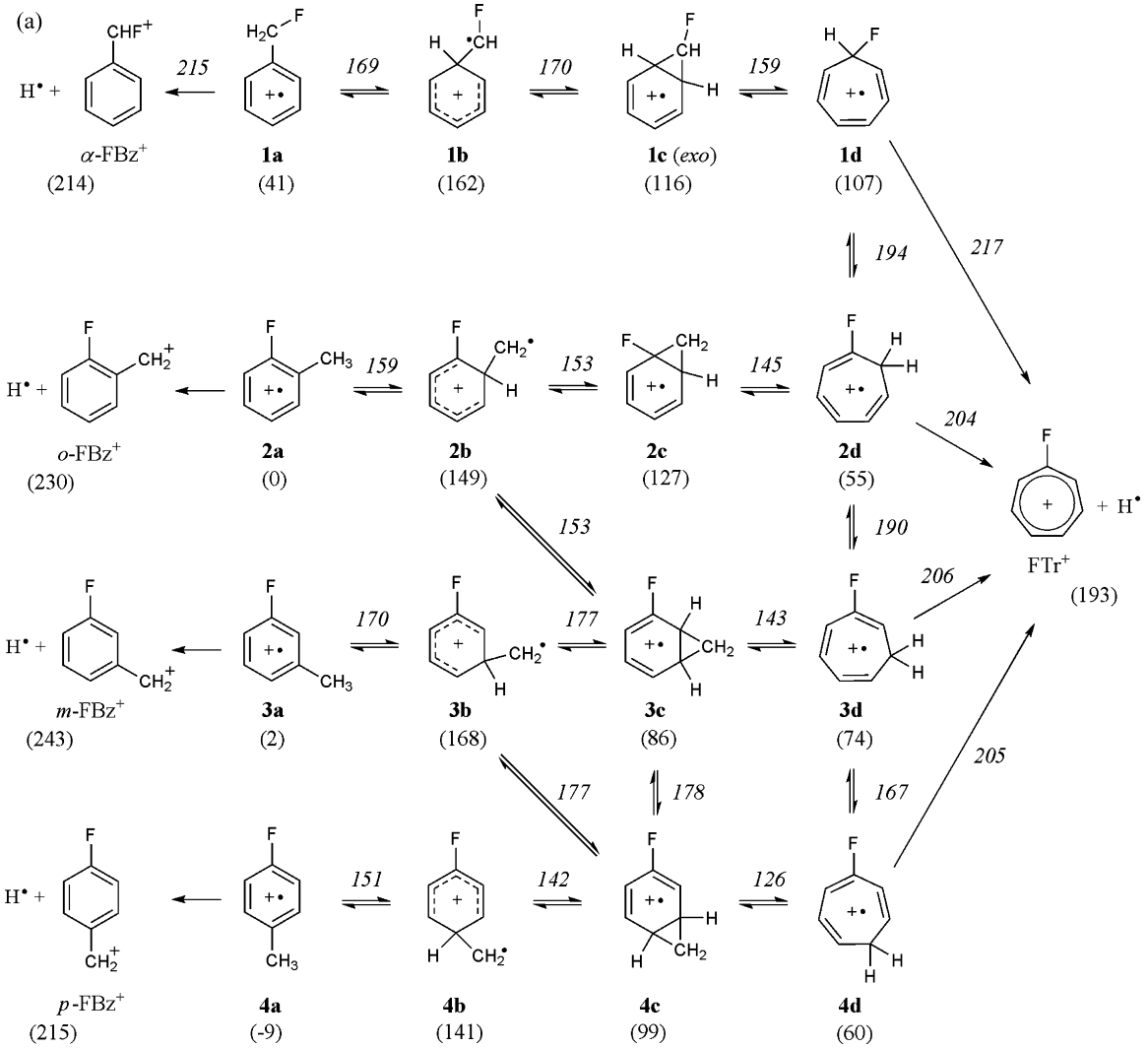

Scheme 1. The isomerization and dissociation pathways of (a) **1a**–**4a** and (b) **1b**–**4b** obtained by B3LYP/6-311 + G(3df,2p)//B3LYP/6-31G(d) calculations. The relative energies (in kJ mol^{-1}) are shown in the parentheses. The values next to the arrows are for the TSs. The ZPVE corrections are included.

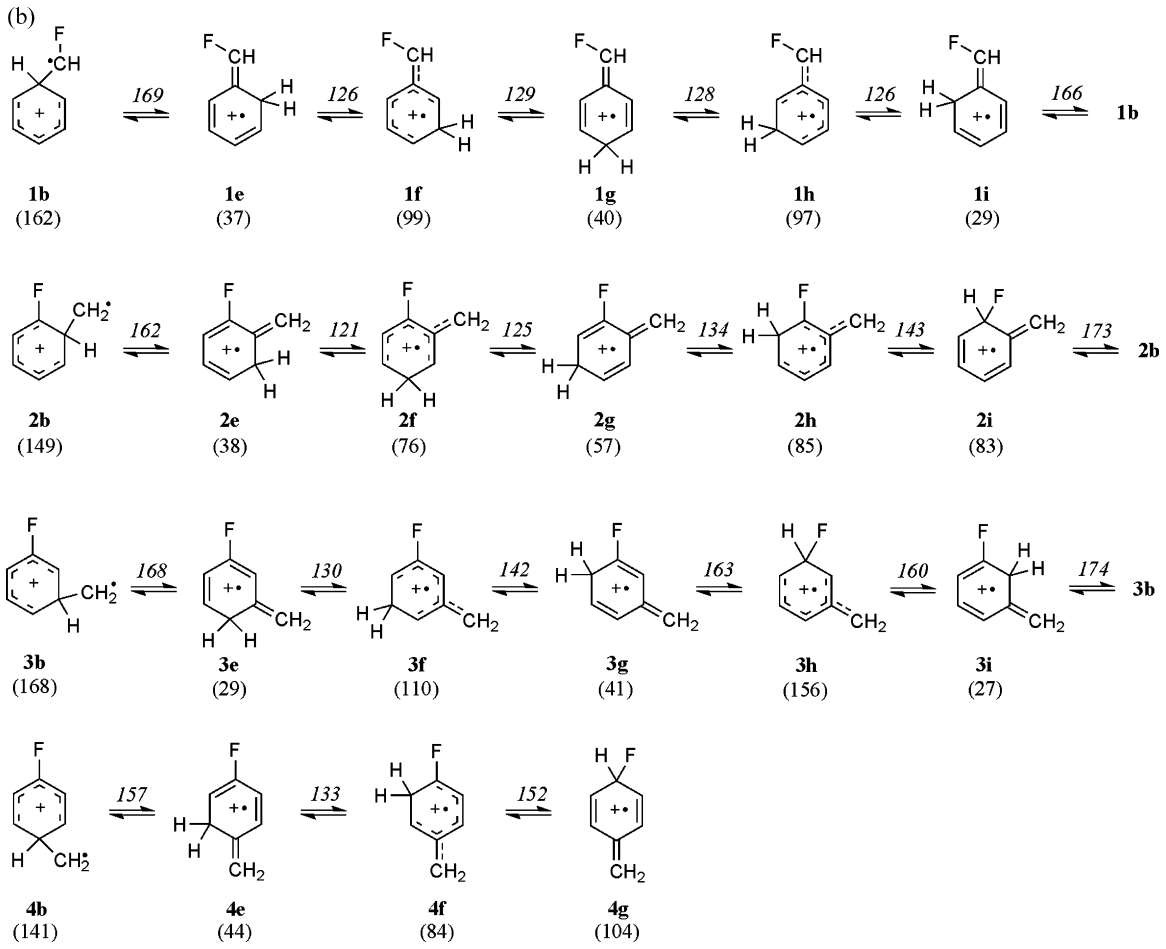

Scheme 1. (*Continued*).

Instead of ring expansion, the four distonic radical cations, **1b**–**4b**, can undergo rearrangements to form a variety of isomers of fluorinated isotoluene ions by the "H-ring walk" mechanism (Scheme 1b). The isomeric fluorinated isotoluene ions can lose H• to form the FBz^+ isomers. The formations of Bz^+ from some of these isomers were energetically less favored than those of FBz^+.

The isomerization between **1a** and **2a** can occur through **1d** and **2d** (Scheme 1a). **2d** can isomerize to **3d** and **4d** by consecutive 1,2-H shift. **2a** can isomerize to **3a** through the "CH_2-ring walk" of **2b** to **3c**, which was energetically more favored than the isomerization through **2d** and **3d**. The isomerization between **3a** and **4a** can occur through the three pathways, **3*b*** ⇄ **4*c***, **3*c*** ⇄ **4*c***, and **3*d*** ⇄ **4*d***. The highest energy barriers in the three isomerization pathways were almost the same (about 175 kJ mol^{-1} higher than **3a**).

Considering only the dissociations of each of **1a**–**4a** by direct C–H bond cleavage and rearrangement by the Hoffman mechanism,

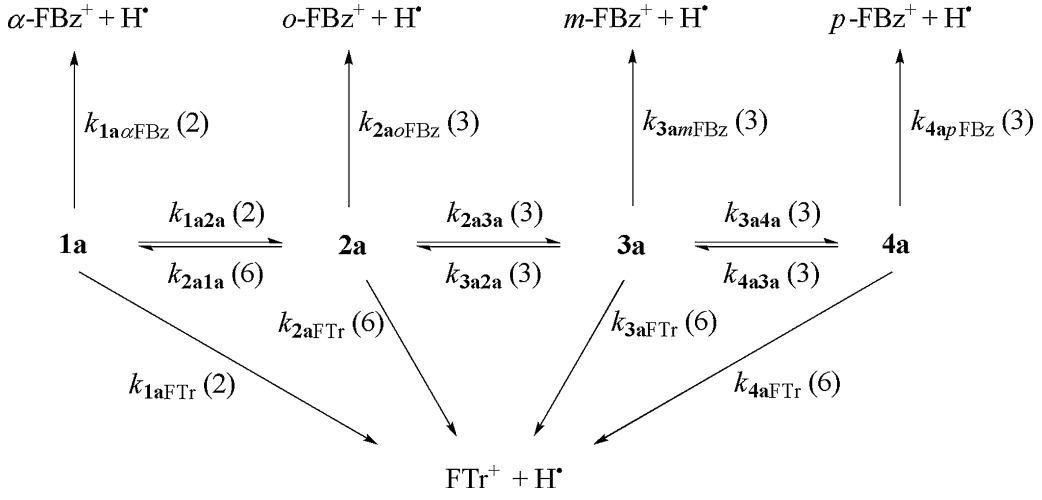

Scheme 2. The simplified reaction pathways of **1a**–**4a**. The reaction path degeneracies used in RRKM calculations are shown in the parentheses next to the *k*'s.

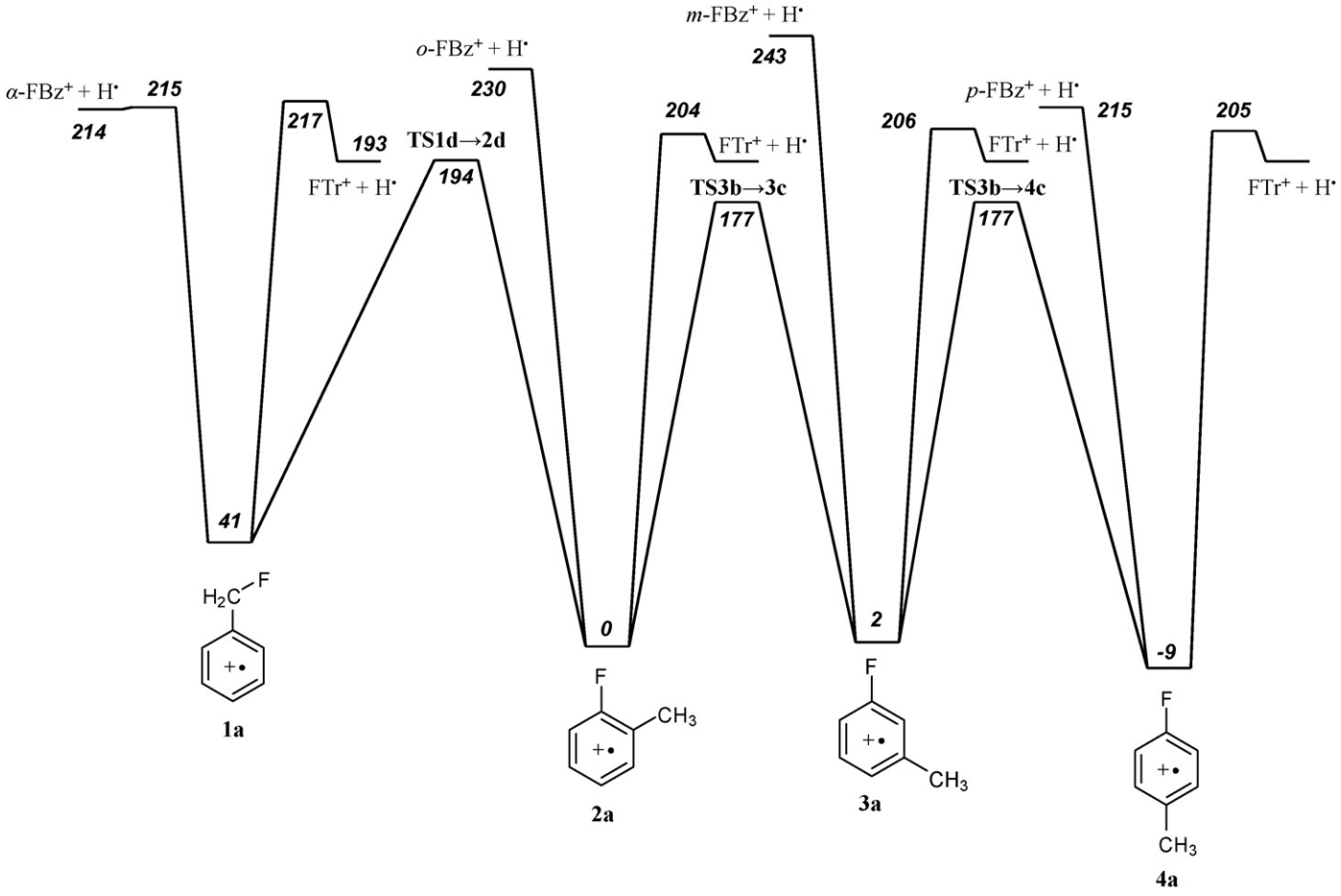

Fig. 1. Potential energy diagram for the isomerization and dissociation of the fluorotoluene ions simplified and derived from the B3LYP/6-311 + G(3df,2p)//B3LYP/6-31G(d) calculations. The italic numbers are the relative energies in kJ mol^{-1}.

the latter is more energetically favored than the former, except in the case of **1a** (Scheme 1a). However, since a rearrangement is entropically less favored than a direct bond cleavage in general, we cannot predict which one is more important in the dissociation kinetics from the potential energy calculations alone. In addition, the isomerizations among the molecular ions make the kinetics more complicated. To examine the competition between the isomerizations and dissociations, the pathways were simplified as shown in Scheme 2. Since the final dissociation steps in the formation of FTr$^+$ from the four molecular ions are the rate-determining steps, the corresponding TSs were chosen as the individual TSs for the simplified one-step dissociations to FTr$^+$ + H$^\bullet$. The simplified PES is shown in Fig. 1. Several isomerization steps between a pair of two fluorotoluene ions were approximated as a single step. TS**1d** → **2d** (denoting TS between **1d** and **2d**), TS**3b** → **3c**, and TS**3b** → **4c** were chosen for the isomerization barriers between **1a** and **2a**, **2a** and **3a**, and **3a** and **4a**, respectively [36]. Their energies were highest in the individual minimum energy reaction pathways between the respective two molecular ions and, hence, they are the rate-determining steps. The pathways through the fluorinated isotoluene ions are not included in the PES, whose contributions to the dissociations will be described later.

The rate constants of the individual reaction steps denoted in Scheme 2 were calculated using the RRKM formula (Eq. (1)). The reaction path degeneracies are denoted in the parentheses next to the *k*'s in Scheme 2. The vibrational frequencies of the reactants and TSs calculated at the B3LYP/6-31G(d) level and scaled by 0.9614 [30] were used. We located a TS (TS**1a** → α-FBz$^+$) for the formation of α-FBz$^+$ by direct C–H bond cleavage from **1a**. Its reverse critical energy was very small (1 kJ mol^{-1}). However, we could not locate the TSs for the formation of the other FBz$^+$ isomers from **2a** to **4a** by direct bond cleavage. So, we assumed that the character of these TSs was similar to that of TS**1a** → α-FBz$^+$. The entropy of activation ($\Delta S^\ddagger$) is often used to characterize the looseness of a TS in RRKM calculations even for a reaction occurring in a microcanonical ensemble [33]. The $\Delta S^\ddagger$ value calculated at 1000 K ($\Delta S^\ddagger_{1000\,K}$) was 6.2 J K^{-1} mol^{-1} for the dissociation through TS**1a** → α-FBz$^+$, which indicates that it occurs through a loose TS. We adjusted the vibrational frequencies of the TSs for the formation of *o*-, *m*-, or *p*-FBz$^+$ from **2a**, **3a**, and **4a**, respectively, so that the $\Delta S^\ddagger_{1000\,K}$ values became 6.2 J K^{-1} mol^{-1}, and used them in the RRKM calculations.

Fig. 2 shows the RRKM rate-energy dependences for the individual reaction steps shown in Scheme 2. First of all, consider the reaction starting from **1a** (Fig. 2a). At low energies of around 200 kJ mol^{-1}, the rate constant for the isomerization to **2a**, $k_{\mathbf{1a2a}}$, is much higher than those for the other steps, i.e., the backward isomerization and the dissociations to α-FBz$^+$ and FTr$^+$. This means that most of the **1a** ions having low energies undergo the isomerization to **2a** prior to their dissociation. The subsequent dissociations will be discussed below. At high energies of around 400 kJ mol^{-1}, however, the rate constant for the isomerization to **2a** is comparable to that for the dissociation to α-FBz$^+$, and is still larger than those for the dissociation to FTr$^+$ and the backward isomerization. This means that about half of the **1a** ions having high energies of around 400 kJ mol^{-1} dissociate to α-FBz$^+$ and that the formation of FTr$^+$ by the rearrangement through the Hoffman mechanism is less favored. Secondly, consider the reaction starting from **2a**

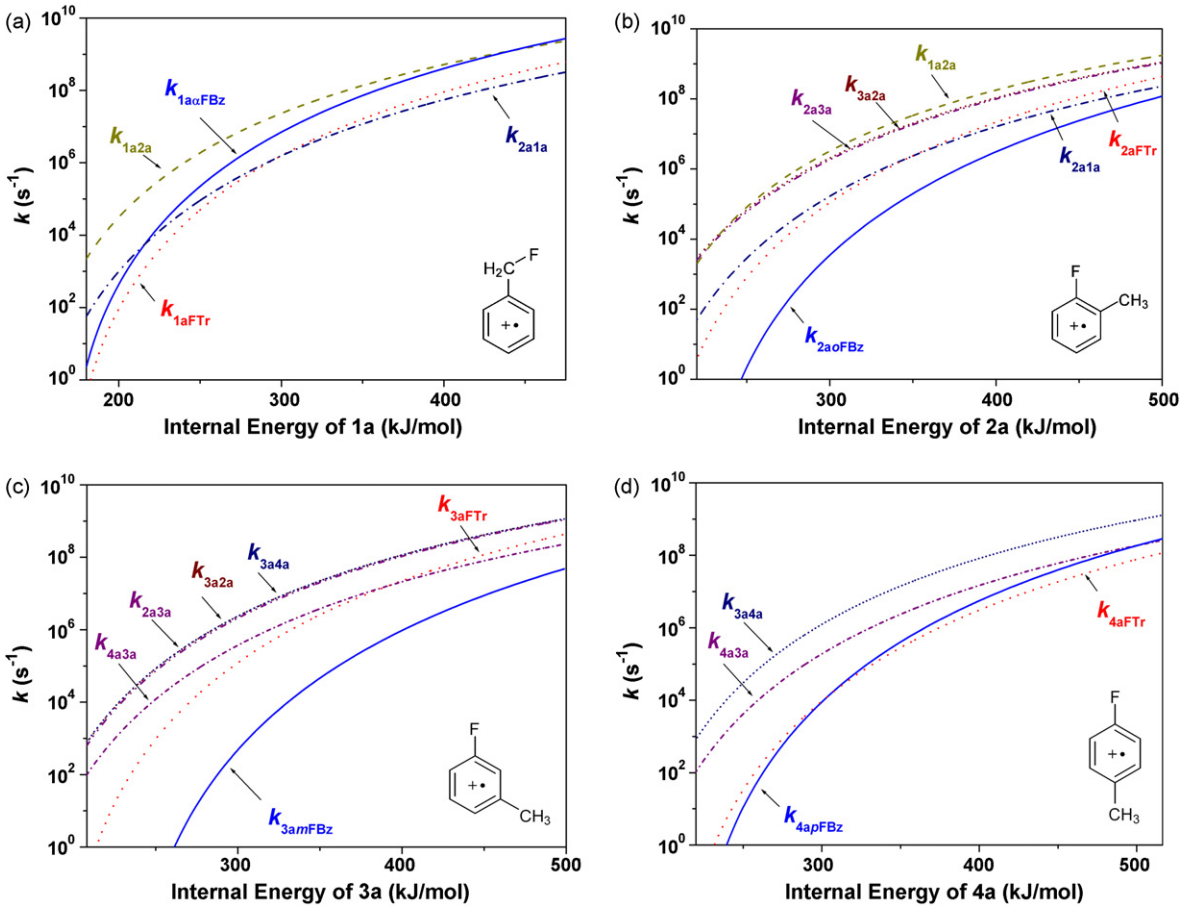

Fig. 2. RRKM rate-energy dependences for the individual reaction channels of (a) **1a**, (b) **2a**, (c) **3a**, and (d) **4a**. $k_{2a3a} \approx k_{3a2a} \approx k_{3a4a}$ in the whole energy range.

(Fig. 2b). The rate constants for the forward and backward isomerizations between **2a** and **3a** are almost the same in the whole energy range calculated. The rate constant for the isomerization to **1a** is smaller than that for the backward isomerization, indicating that the isomerization **2a** → **1a** is less important. The rate constants for the dissociation steps are much smaller than those for the isomerization to **3a** at low energies. As the energy increases, their differences become smaller. This means that about half of the **2a** ions isomerize to **3a** prior to their dissociation at low energies, and the dissociation to FTr^+ can increasingly compete with the isomerization as the energy increases. Thirdly, consider the reaction starting from **3a**. Fig. 2c shows that the rate constants for the isomerizations **3a** → **2a**, **3a** → **4a**, and **2a** → **3a** are almost the same and that they are larger than those for the isomerization **4a** → **3a** and for the dissociations. This means that a large portion of the **3a** ions isomerize to **4a** prior to their dissociation, especially at low energies. Similar to the reaction starting from **2a**, the dissociation channel to FTr^+ becomes increasingly competitive with the isomerizations as the energy increases. Finally, consider the reaction starting from **4a** (Fig. 2d). The rate constant for the isomerization to **3a** is smaller than that for the backward isomerization, reflecting the better stability of **4a** compared to that of **3a**. At low energies, these isomerizations occur much faster than the dissociations, whereas at high energies the dissociations can compete with the isomerizations.

To summarize the individual reaction kinetics described so far, at low energies **2a**, **3a**, and **4a** are interconvertible prior to dissociation and most of the **1a** ions isomerize to **2a**. At high energies, the dissociations can compete with the interconversion. To predict the overall dissociation rates of **2a**, **3a**, and **4a**, we assumed that their isomerizations were very fast compared to their dissociations, which is quite valid for the ions having low energies. In this case, we should consider a pool of reactants consisting of **2a**, **3a**, and **4a** in the RRKM calculation for the dissociations of the individual molecular ions. Therefore, the sum of their densities of states, $\rho_{2a} + \rho_{3a} + \rho_{4a}$, was used in the rate calculations (Eq. (1)) [33]. The resultant rate-energy dependences (Fig. 3) show that the formations of *o*- and *m*-FBz^+ occur much more slowly than the other dissociations. The three dissociation channels to FTr^+ via **2d**, **3d**, and **4d** contributed almost equally to the formation of FTr^+ (not shown in Fig. 3). The

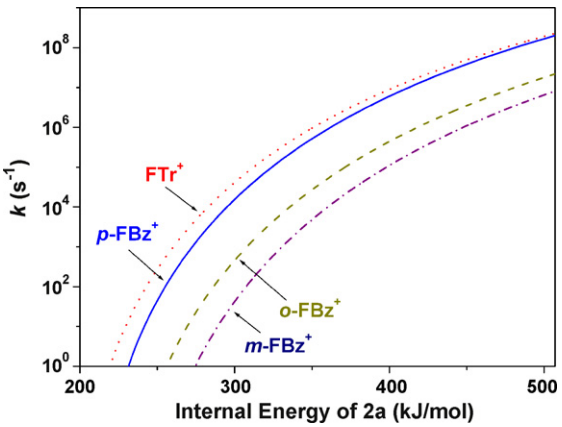

Fig. 3. RRKM rate-energy dependences for the formations of $C_7H_6F^+$ isomers from a pool of **2a**–**4a**. The product $C_7H_6F^+$ isomers are denoted. It was assumed that the interconversion among **2a**–**4a** was much faster than the dissociations.

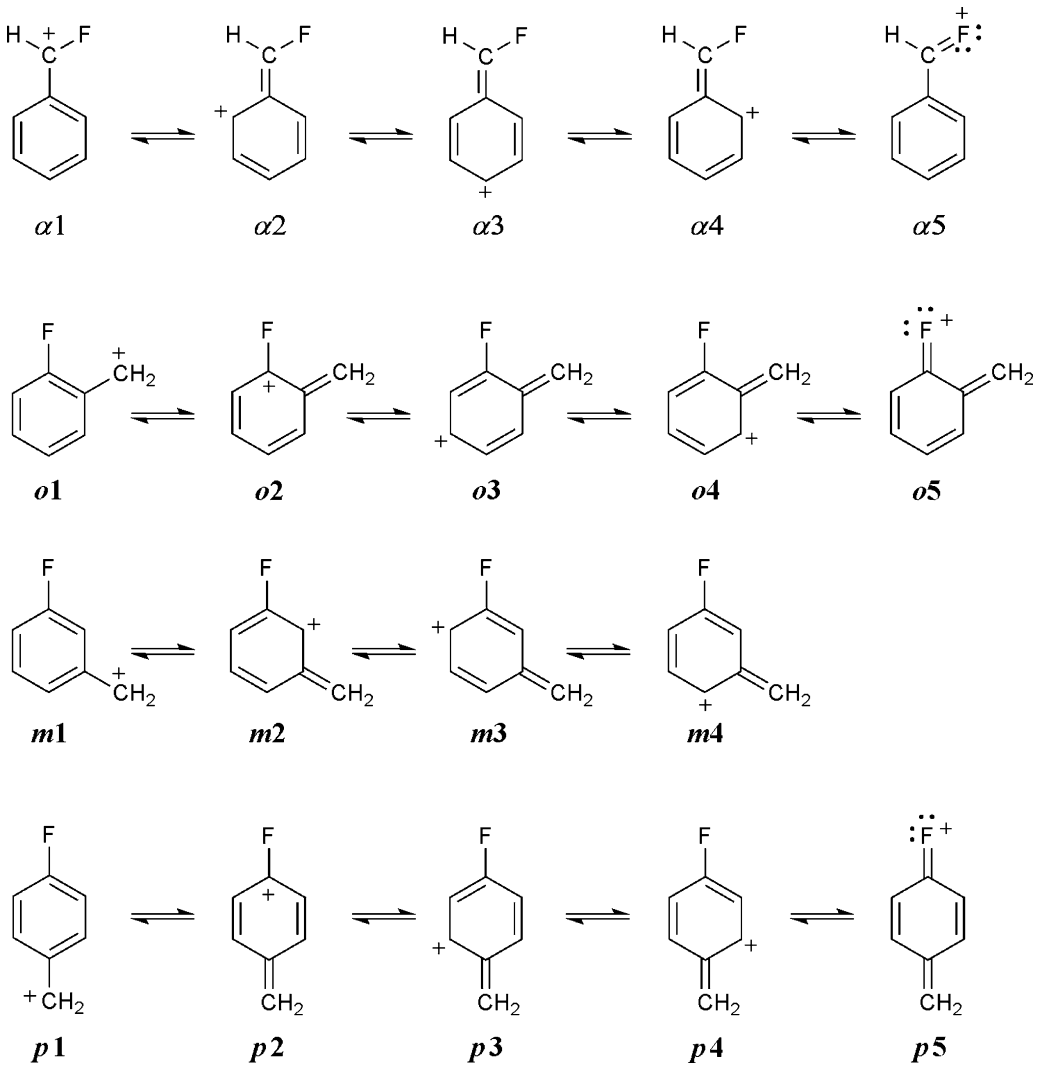

Scheme 3.

sum of the three contributions to the formation of FTr^+ dominates near the dissociation threshold and as the energy increases the formation of *p*-FBz^+ becomes more competitive. Because the formation of $C_7H_6F^+$ isomers occurs competitively, the sum of their rate constants becomes the overall dissociation rate constant of the molecular ions.

Jackson et al. [4] measured the FTr^+/FBz^+ branching ratios as a function of the energy of the ionizing electrons for the dissociation of **2a**, **3a**, and **4a**. The electron energy varied from 14 to 25 eV. The $C_7H_6F^+$ ions formed from *o*-, *m*-, and *p*-fluorotoluene were reacted with *p*-diethylbenzene in an ion cyclotron resonance spectrometer. They assumed that FBz^+ was reactive, whereas FTr^+ was unreactive, as in the case of the two fractions (Bz^+ and Tr^+) observed for the $C_7H_7^+$ ions. The opposite behavior in the latter case has been well accepted. The abundances of FTr^+ ions in all of the ortho, meta, and para isomers decreased with increasing energy, but their absolute values at the same energies were similar for the different isomers. This tendency agrees with the present kinetic analysis described above, but not quantitatively. The experimental fractions of FTr^+ are between 40 and 30%, whereas the present theoretical ones are larger than 50%. This quantitative disagreement can be reduced by considering some factors ignored in the approximations made in the RRKM calculation. First of all, we ignored the formation of FBz^+ through the fluorinated isotoluene ions. Actually, the contributions would not be as large as that from the direct loss of $H^\bullet$ from **4a**. For example, the TSs for the formation of *p*-FBz^+ from **4e** and **4g** lay higher than that from **4a** by 7 and 12 kJ mol^{-1} [37], respectively, and were tighter. However, these channels can contribute to the formation of FBz^+ to some extent. Secondly, some of the **2a**, **3a**, and **4a** ions can isomerize to **1a** prior to their direct dissociation and undergo dissociation mainly to α-FBz^+, especially at high energies. Finally, the assumption made to calculate the rate-energy dependences in Fig. 3 is not entirely valid at high energies. The isomerizations **2*a*** ⇄ **3*a*** and **3a** → **4a** are faster than the dissociations, but the rates for the isomerization **4a** → **3a** are comparable with those for the dissociations at high energies (Fig. 2). This means that the channels for the formation of FTr^+ through **2d** and **3d** would contribute less than the above prediction at high energies. All of these three factors make the fractions of FTr^+ become less than the above prediction.

The ionization energies (IEs) of the fluorotoluene isomers and appearance energies (AEs) of the $C_7H_6F^+$ fragments in electron ionization mass spectrometry were reported [27]. The difference between appearance and ionization energy, AE − IE, is the minimum energy to form the fragment ion in the ionization source. It is usually larger than the critical energy for the dissociation due to the kinetic shift [38]. The reported values of AE − IE for **2a**–**4a** are in the range 290–330 kJ mol^{-1}. The result shown in Fig. 3 predicts that the dissociation rate constants of the molecular ions having these energies are in the range 10^5 to 10^6 s^{-1}, which agrees well with a

Table 1
The calculated G3//B3LYP energies and BDEs of some species in kJ mol^{-1}.

Reaction	Relative energy[a]		BDE[c]
	Reactant	Products (FBz^+)[b]	
1a → *α*-FBz^+ + H•	42.0	211.6 (−12.9)	169.6
2a → *o*-FBz^+ + H•	0.0	224.5 (0.0)	224.5
3a → *m*-FBz^+ + H•	3.4	238.1 (13.5)	234.7
4a → *p*-FBz^+ + H•	−5.3	209.9 (−14.6)	215.2
$TOL^{+\bullet} \rightarrow Bz^+ + H^\bullet$			216[d]

[a] Relative to **2a**. The calculated total energies of **2a** and H• are −370.2144000 and −0.5010870 hartrees, respectively.
[b] The values in the parentheses are the energies of the FBz^+ isomers relative to *o*-FBz^+.
[c] BDE(C–H) of the CH_2F or CH_3 group.
[d] Ref. [26].

rate corresponding to the maximum ion lifetime in the source of conventional mass spectrometry.

The main dissociation channel of **1a** would be dependent on its energy. At low energies most of the **1a** ions isomerized to **2a** prior to their dissociation as mentioned above. The dissociation after the isomerization would be similar to that starting from **2a**, of which the main products were FTr^+ and *p*-FBz^+. Since at high energies, however, the dissociation to *α*-FBz^+ was competitive with the isomerization to **1a**, *α*-FBz^+ would be another major dissociation product.

The isomerization pathways of **1a**–**4a** are similar to those of the chloro-, bromo-, and iodotoluene ions reported recently [15,16]. In their dissociations, however, there is a striking difference, in that the fluorotoluene ions mainly lose H•, whereas the other halotoluene ions mainly lose X•. This is attributed to the high C–F bond energy as mentioned in Section 1. The energetics of the isomerization and dissociation of the fluorotoluene ions are similar to those of $TOL^{+\bullet}$. In the reported PES of the dissociation of $TOL^{+\bullet}$ [26], the direct C–H bond cleavage step lies higher than the barriers for the rearrangements, which eventually lead to the formation of Bz^+ and Tr^+, respectively. In the dissociations of the isomeric fluorotoluene molecular ions, the direct C–H bond cleavage steps lie higher than the rearrangement steps except for the dissociation of **1a** in which their energies were similar. On the other hand, in the reported PESs for the dissociations of the *α*-isomers of the chloro-, bromo-, and iodotoluene ions [15,16], the direct C–X bond cleavage steps lie lower than the rearrangement steps leading to the formation of Tr^+. Due to this difference in energetics, Tr^+ is not one of the major $C_7H_7^+$ products in the dissociation of these halotoluene ions, whereas Tr^+ or FTr^+ is included in the major products in the dissociations of $TOL^{+\bullet}$ or fluorotoluene ions, respectively. The labile C–X (X = Cl, Br, I) bond is responsible for the predominant formation of Bz^+ from chloro-, bromo-, and iodotoluene ions.

The endoergicities for the formation of FBz^+ from **1a**–**4a** by direct C–H bond cleavages, i.e., the BDEs, were different, indicating that the position of F affects the BDE(C–H). To compare them more accurately, G3//B3LYP calculations were carried out for **1a**–**4a** and the four isomers of FBz^+. Their relative energies and BDEs are listed in Table 1 together with the data for the formation of Bz^+ from $TOL^{+\bullet}$. The relative G3//B3LYP energies agreed with the B3LYP/6-311 + G(3df,2p)//B3LYP/6-31G(d) values within ±4 kJ mol^{-1}. The calculated BDE(C–H) of **1a** was much smaller than that of $TOL^{+\bullet}$, while that of **4a** was similar to that of $TOL^{+\bullet}$ and those of **2a** and **3a** were larger. The stability of both the reactant and product ions should be considered when discussing the trend of the BDE. The energies of **2a**, **3a**, and **4a** were similar, but **1a** was much less stable than the other isomers. The substitution position selectivity of the stability can be easily understood by using familiar valence bond (VB) concepts. The resonance stability is enhanced to a great extent by a fluorine substitution at the aromatic ring of $TOL^{+\bullet}$ than at the CH_3 group. The lone pair electrons of F at the CH_2F group cannot contribute to the resonance stability. This makes **1a** less stable than the other isomers. Upon the loss of H•, the relative stability changes remarkably. The alpha and para FBz^+ isomers are more stable than the ortho isomer, and the meta isomer is the least stable. The possible reasonable resonance structures for the FBz^+ isomers are drawn in Scheme 3. The stabilization by the former four forms (***x*1**–***x*4**, ***x*** = ***α***, ***o***, ***m***, or ***p***) is similar for the four FBz^+ isomers except for the para isomer. Since ***p*3** and ***p*4** are equivalent contributors, the para isomer is stabilized more than the other isomers when considering only these four resonance forms. The alpha, ortho, and para isomers have additional resonance forms (***α*5**, ***o*5**, and ***p*5**) in which the positive charge is stabilized by the donation of an electron pair from F. The meta isomer has no such additional stabilization. This accounts for its having the least stability. Since the aromaticity is preserved in ***α*5**, the alpha isomer should be more stable than the ortho isomer. Compared to the ortho isomer, the para isomer has additional stabilization originating from the equivalency of ***p*3** and ***p*4** as described above.

4. Conclusion

The DFT calculations showed that the isomerization barriers among **1a4a** lay below the dissociation barriers. The RRKM model calculation predicts that at low energies **2a**, **3a**, and **4a** are interconvertible prior to their dissociation, which is different from the dissociation behavior of the other halotoluene molecular ions reported previously. At high energies, the dissociation channels can compete with the interconversion. The main $C_7H_6F^+$ products in the dissociations of **2a**, **3a**, and **4a** were FTr^+ and *p*-FBz^+. It is predicted that at low energies most of the **1a** ions isomerize to **2a** and the subsequent reactions are the same as those of **2a**. As the energy increases, the dissociation to *α*-FBz^+ would become more important, because it can begin to compete with the isomerization to **2a**. The comparison with the experiments carried by the method based on electron ionization has the limit of definition of internal energy. Further experimental studies on the molecular ions having well-defined internal energies will be helpful in deeper understanding of their dissociation mechanisms and kinetics.

From the MO calculations we could observe that the position of F affects the BDE(C–H) of the methyl group. This is attributed to the differences in the stability of **1a**–**4a** and the four FBz^+ isomers which could be well understood by the VB theory.

Acknowledgements

The author wishes to thank Professor Hongbum Kim for valuable discussion and Eun Sil Kim for assistance in the theoretical calculations. This work was supported by a Korea Research Foundation Grant funded by the Korean Government (MOEHRD) (KRF-2008-313-C00403). The author would like to acknowledge the support from the KISTI Supercomputing Center (KSC-2008-S01-0010).

References

[1] F.W. McLafferty, J. Winkler, J. Am. Chem. Soc. 96 (1974) 5182.
[2] F.W. McLafferty, F.M. Bockhoff, J. Am. Chem. Soc. 101 (1979) 1783.
[3] G. Bouchoux, Org. Mass Spectrom. 12 (1977) 681.
[4] J.A.A. Jackson, S.G. Lias, P. Ausloos, J. Am. Chem. Soc. 99 (1977) 7515.
[5] T. Baer, B.P. Tsai, D. Smith, P.T. Murray, J. Chem. Phys. 64 (1976) 2460.
[6] T. Baer, J.C. Morrow, J.D. Shao, S. Olesik, J. Am. Chem. Soc. 110 (1988) 5633.
[7] S. Olesik, T. Baer, J.C. Morrow, J.J. Ridal, J. Buschek, J.L. Holmes, Org. Mass Spectrom. 24 (1989) 1008.
[8] E.W. Fu, P.P. Dymerski, R.C. Dunbar, J. Am. Chem. Soc. 98 (1975) 337.
[9] R.C. Dunbar, J.P. Honovich, B. Asamoto, J. Phys. Chem. 92 (1988) 6935.
[10] C.Y. Lin, R.C. Dunbar, J. Phys. Chem. 98 (1994) 1369.
[11] C. Lifshitz, I. Levin, S. Kababia, R.C. Dunbar, J. Phys. Chem. 95 (1991) 1667.
[12] J.C. Traeger, B.M. Kompe, Int. J. Mass Spectrom. Ion Process. 101 (1990) 111.
[13] J.C. Choe, M.S. Kim, Int. J. Mass Spectrom. Ion Process. 107 (1991) 103.

[14] Y.S. Cho, M.S. Kim, J.C. Choe, Int. J. Mass Spectrom. Ion Process. 145 (1995) 187.
[15] J.C. Choe, J. Phys. Chem. A 112 (2008) 6190.
[16] J.C. Choe, Int. J. Mass Spectrom. 278 (2008) 50.
[17] S.K. Shin, S.J. Han, B. Kim, Int. J. Mass Spectrom. Ion Process. 157 (1996) 345.
[18] B. Kim, S.K. Shin, J. Chem. Phys. 106 (1997) 1411.
[19] B. Kim, S.K. Shin, J. Phys. Chem. A 106 (2002) 9918.
[20] S.K. Shin, B. Kim, R.L. Jarek, S.J. Han, Bull. Kor. Chem. Soc. 23 (2002) 267.
[21] S.-J. Kim, C.-H. Shin, S.K. Shin, Mol. Phys. 105 (2007) 2541.
[22] J. Seo, H.-I. Seo, S.-J. Kim, S.K. Shin, J. Phys. Chem. A 112 (2008) 6877.
[23] S.K. Shin, S.-J. Han, J. Seo, Int. J. Mass Spectrom. 283 (2009) 185.
[24] C. Lifshitz, Y. Gotkis, A. Ioffe, J. Laskin, S. Shaik, Int. J. Mass Spectrom. Ion Process. 125 (1993) 7.
[25] C. Lifshitz, Acc. Chem. Res. 27 (1994) 138.
[26] J.C. Choe, J. Phys. Chem. A 110 (2006) 7655.
[27] NIST Chemistry WebBook, NIST Standard Reference Database Number 69, In: P.J. Linstrom, W.G. Mallard (Eds.).
[28] M.J. Frisch, G.W. Trucks, H.B. Schlegel, G.E. Scuseria, M.A. Robb, J.R. Cheeseman, J.A. Montgomery Jr., T. Vreven, K.N. Kudin, J.C. Burant, J.M. Millam, S.S. Iyengar, J. Tomasi, V. Barone, B. Mennucci, M. Cossi, G. Scalmani, N. Rega, G.A. Petersson, H. Nakatsuji, M. Hada, M. Ehara, K. Toyota, R. Fukuda, J. Hasegawa, M. Ishida, T. Nakajima, Y. Honda, O. Kitao, H. Nakai, M. Klene, X. Li, J.E. Knox, H.P. Hratchian, J.B. Cross, V. Bakken, C. Adamo, J. Jaramillo, R. Gomperts, R.E. Stratmann, O. Yazyev, A.J. Austin, R. Cammi, C. Pomelli, J.W. Ochterski, P.Y. Ayala, K. Morokuma, G.A. Voth, P. Salvador, J.J. Dannenberg, V.G. Zakrzewski, S. Dapprich, A.D. Daniels, M.C. Strain, O. Farkas, D.K. Malick, A.D. Rabuck, K. Raghavachari, J.B. Foresman, J.V. Ortiz, Q. Cui, A.G. Baboul, S. Clifford, J. Cioslowski, B.B. Stefanov, G. Liu, A. Liashenko, P. Piskorz, I. Komaromi, R.L. Martin, D.J. Fox, T. Keith, M.A. Al-Laham, C.Y. Peng, A. Nanayakkara, M. Challacombe, P.M.W. Gill, B. Johnson, W. Chen, M.W. Wong, C. Gonzalez, J.A. Pople, Gaussian 03, Revision C. 02, Gaussian, Inc., Wallingford, CT, 2004.
[29] M.W. Wong, L. Radom, J. Phys. Chem. A 102 (1998) 2237.
[30] A.P. Scott, L. Radom, J. Phys. Chem. A 100 (1996) 16502.
[31] A.G. Baboul, L.A. Curtiss, P.C. Redfern, J. Chem. Phys. 110 (1999) 7650.
[32] L.A. Curtiss, K. Raghavachari, P.C. Redfern, V. Rassolov, J.A. Pople, J. Chem. Phys. 109 (1998) 7764.
[33] T. Baer, W.L. Hase, Unimolecular Reaction Dynamics: Theory and Experiments, Oxford, New York, 1996.
[34] T. Beyer, D.R. Swinehart, ACM Commun. 16 (1973) 379.
[35] M.K.Z. Hoffman, Z. Naturforsch. 29a (1974) 1077.
[36] It is estimated that the approximation of choice of one TS for the rate-determining step underestimates the rate constants of the forward and reverse isomerization between **2a** and **3a** by a factor of two. However, this does not affect the results of the present kinetic analysis.
[37] Even though the energy differences are close to the uncertainty of the present calculations, the presence of the reverse barriers, meaning tighter TSs, makes these channels still less important than the direct H$^{\bullet}$ loss from **4a**.
[38] K. Levsen, Fundamental Aspects of Organic Mass Spectrometry, Verlag Chemie, Weinheim, 1978.